

P014 ELEMENTS OF CALIBRATION AND DATA INTERPRETATION OF EMI SOUNDING DEVICE EMS

E.V. BALKOV, M.I. EPOV, A.K. MANSTEIN, Y.A. MANSTEIN

Institute of Geophysics, Siberian Branch of Russian Academy, 630090 Russia, Novosibirsk, Koptyuga str, 3

Present work is devoted to development of mathematical apparatus for calibration, data processing, inversion and visualization of electromagnetic induction sounding device EMS. Mathematical algorithms, results of modeling and its practical use will be presented in the contribution.

Introduction Electromagnetic induction frequency sounding device EMS (Figure 1a) is the portable shallow-depth prospecting device for hand-held or vehicular exploration of apparent conductivity distribution in the ground. It can be used for vary applications in engineering geophysics, archaeology and environmental monitoring.

a)



b)

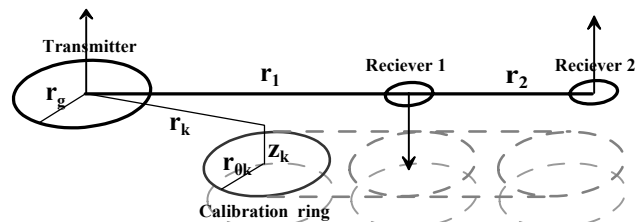


Fig. 1. (a) EMS and operator view. (b) Scheme of EMS device and placement of calibration ring.

EMS device is the three-coil sonde that includes the transmitter and two receivers (Figure 1b). Alternating magnetic field with controllable phase is generating consequently on several frequencies within the range from 2.5 to 200 kHz. Receivers have special geometry to compensate primary field in the air. So EMS registers differential electromotive force induced by secondary sources.

For some practical problems (e.g. determination of location of long linear conductive objects such as pipes and cables) it is enough to have the EMS data set representing distribution of pure signal within area under exploration site. However for a wide range of application (e.g. determination of resistivity distribution, location of high-salinity soils and contaminated groundwater etc.) it must be developed corresponding mathematical and program apparatus for data calibration for each used frequency, calculation of apparent resistivity and 1D inversion of EMS data to the layered earth.

Calibration and interpretation System including EMS device and wire cuprous loop was chosen as calibration model. The ring can be moved at the plain that is parallel to the plain of transmitter (Figure 1b).

Mathematical model is described by Maxwell system with appropriate bound conditions.

$$\begin{cases} \text{rot}H = (\sigma + i\omega\mu\varepsilon)E & \text{div}H = 0 \\ \text{rot}E = -i\omega\mu H & \text{div}E = 0 \end{cases}$$

It was obtained expressions for vertical component of magnetic field and tangential component of electrical field for the case of field exciting by magnetic dipole and current ring

$$H_z = -\frac{M_g}{4\pi R^3} (\sin^2 \theta (3 + 3kR + k^2 R^2) - 2 - 2kR) e^{-kR}; E_\phi = -i\omega\mu \frac{M_g \sin \theta}{4\pi R^2} (1 + kR) e^{-kR},$$

$$H_z = \frac{1}{r} \frac{I_g r_g}{4\pi} \int_0^{2\pi} \frac{e^{-kR_l}}{R_l} \cos \alpha d\alpha + \frac{I_g r_g}{4\pi} \int_0^{2\pi} \cos \alpha (r_g \cos \alpha - r) (1 + kR_l) \frac{e^{-kR_l}}{R_l^3} d\alpha,$$

$$E_\phi = -i\omega\mu \frac{I_g r_g}{4\pi} \int_0^{2\pi} \frac{e^{-kR_l}}{R_l} \cos \alpha d\alpha; k^2 = i\omega\mu\sigma - \omega^2 \varepsilon\mu.$$

in homogeneous media.

Analytical expressions for magnetic dipole are more clear and convenient for analysis. That is why the mathematical modeling was carried out. It allows determining the areas where EMS transmitter can be approximated by magnetic dipole (Figure 2a, 2b). Blue zones correspond to the values of approximation error that is less than 1 percent.

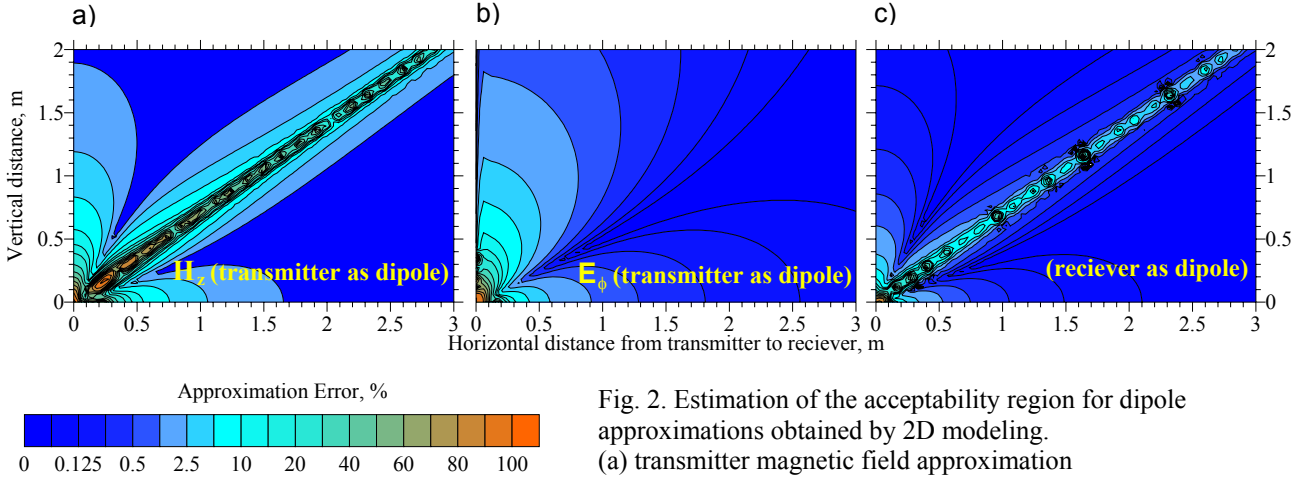


Fig. 2. Estimation of the acceptability region for dipole approximations obtained by 2D modeling.
(a) transmitter magnetic field approximation
(b) transmitter electrical field approximation
(c) receiver approximation

Also it was derived expressions for electromotive force induced in receiver which can have finite size (e.g. for calibration ring) and can be dipole (e.g. for EMS receivers).

$$\varepsilon = r_{0k} \int_0^{2\pi} E_\phi [x(\psi), y(\psi), z(\psi)] [\sin(\varphi(\psi)) \sin(\psi) + \cos(\varphi(\psi)) \cos(\psi)] d\psi,$$

$$\varepsilon = -i\omega\mu M_k H_z \Big|_{r=r_k, z=z_k},$$

where M_g, I_g, r_g is the momentum, current and radius of the transmitter respectively; M_k, r_{0k} - momentum and radius of the receiver respectively. Estimation of dipole approximation was obtained. Results are presented at Figure 2c.

A series of calibration experiments was performed, where calibration ring was moved in horizontal plane at different distance (z_k) from the sonde. Sample results at particular frequency are presented at Figure 3. It shows the dependences of inphase and quadrature components of experimental and synthetic data from the horizontal position of calibration ring while the height is fixed. There were obtained correction factors at each frequency and phase

characteristic was examined. The relative correlation of experimental and synthetic data is not less than 5 percent.

It is well known that quadrature component of EM signal is proportional to the conductivity of conductive homogeneous half space when frequency and conductivity have quite small values (low-frequency approximation). The full expression of electromotive force induced in EMS receivers is printed below.

$$\varepsilon = -i\omega\mu_0 \frac{M_g}{2\pi k^2} \left\{ \frac{M_1}{r_1^5} \left[9 - (9 - ikr_1 - 4k^2 r_1^2 + ik^3 r_1^3) e^{ikr_1} \right] + \frac{M_2}{r_2^5} \left[9 - (9 - ikr_2 - 4k^2 r_2^2 + ik^3 r_2^3) e^{ikr_2} \right] \right\}.$$

Analysis shows that low-frequency approximation is not valid for considered frequency and resistivity ranges. Because of that it is necessary to solve transcendental equation which equal expression presented below where left-hand member is the experimental electromotive force. Because of ambiguity of the function it is necessary to choose the ranges of monotony that is possible at fixed range of conductivity and with several frequencies. Such transform gives the values of conductivity at different frequencies under the model of homogeneous half space. This values is conventional called as apparent conductivity and give the approximate representation of the real conductivity distribution.

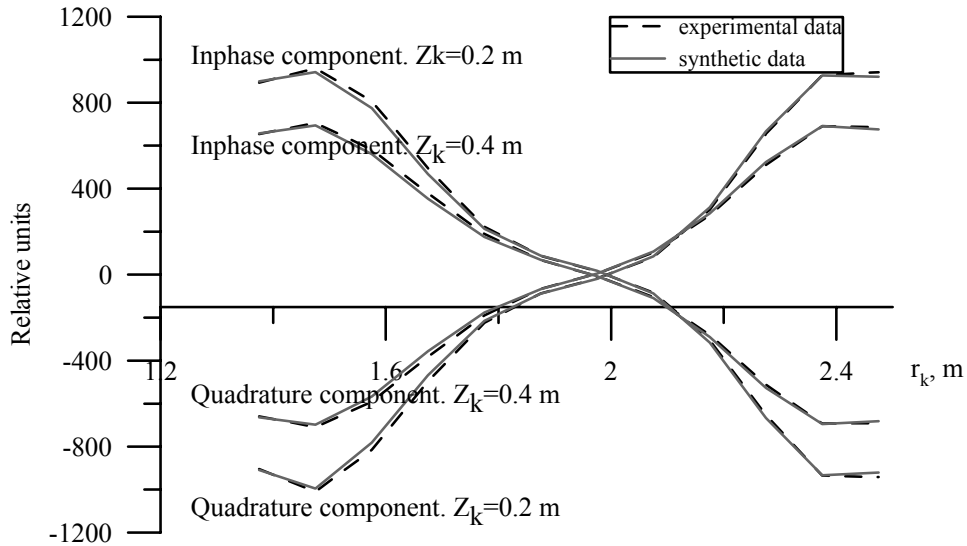


Fig. 3. Experimental and synthetic data comparison.

In some cases we can use apparent resistivity values as the final result of interpretation but to derive more precise information about the distribution of resistivity with depth changes it is need to perform at least 1D inversion procedure. The horizontally layered earth local model was accepted. The formulas for forward problem are following.

$$H_z = \frac{M_g}{2\pi} \int_0^{\infty} \lambda^3 J_0(\lambda r) X d\lambda; \quad E_{\varphi} = -\frac{i\omega\mu_0 M_g}{2\pi} \int_0^{\infty} \lambda^2 J_1(\lambda r) X d\lambda,$$

$$X = \frac{f_{l+0}}{f_{l-0} h_{l+0} - f_{l+0} h_{l-0}} \zeta(z), z < z_l; \quad X = \frac{f_{l-0}}{f_{l-0} h_{l+0} - f_{l+0} h_{l-0}} \zeta(z), z > z_l,$$

$$\varepsilon = i\omega\mu_0 (M_1 H_z(r_1) - M_2 H_z(r_2)),$$

where X – the layered media function, z_l – the boundary which include the field source, $f = \mu\zeta$, $h = \zeta'_z$, the function $\zeta(z)$ is calculated using recursive algorithm from its boundary values ($\zeta_n(z) = \zeta(z_n)$, $n = 0 \dots N$), N – number of layers, $p_n = \lambda^2 + k_n^2$, $k_n^2 = i\omega\mu\sigma$, $n = 0 \dots N$.

$$\zeta(z) = \zeta_{1-0} e^{p_0(z-z_1)}, z \leq z_0; \zeta(z) = \zeta_{n+0} ch(p_n(z-z_n)) + \zeta'_{n+0} \frac{sh(p_n(z-z_n))}{p_n},$$

$$\zeta(z) = \zeta_{n+1-0} ch(p_n(z-z_{n+1})) + \zeta'_{n+1-0} \frac{sh(p_n(z-z_{n+1}))}{p_n}; \zeta(z) = \zeta_{N+0} e^{-p_N(z-z_N)}, z \geq z_N.$$

Inversion algorithm is based on minimization of the objective function using the method developed by Nelder and Mead. Objective function has the following form.

$$F = \sqrt{\sum_{k=1}^N \left(\frac{\varepsilon^{\text{exp}} - \varepsilon^{\text{synth}}}{\sigma \varepsilon^{\text{synth}}} \right)^2},$$

where N – the number of the layers, ε^{exp} , $\varepsilon^{\text{synth}}$, $\sigma \varepsilon^{\text{synth}}$ – experimental and synthetic electromotive force and dispersion of experimental data respectively.

Case study EMS device, its mathematical algorithms and program software was tested at numerous sites in Russia, Italy and Antarctica. Figure 4 demonstrates example of express interpretation (transformation to the apparent resistivity) of field data obtained at archaeological site. Ambient structures such as trench and foundation can be seen at the charts which correspond to various depth of exploration.

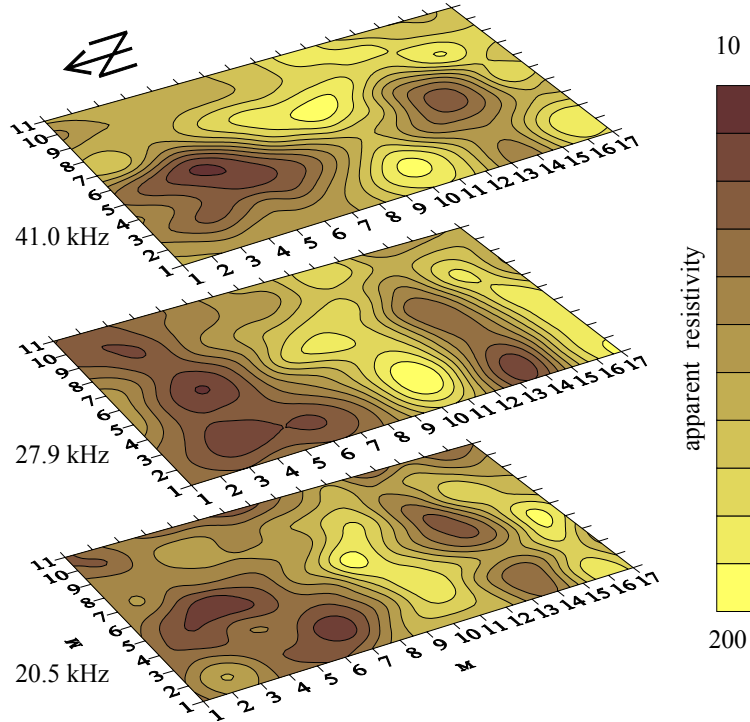


Fig. 4. Express interpretation of field data.

Conclusion Mathematical and program apparatus for EMS calibration, calculation of apparent resistivity and 1D inversion of EMS data to the layered earth was developed and tested at numerous experiments.

Acknowledgements Investigations were carried out under the financial support of Russian Fund of Basic Research. Grants: #00-06-80412, #02-06-06041, #03-06-80415.